DFT-Spread OFDM Joint Radar-Communication System

Dylan Boland (Student)

***Abstract*—In wireless communications, orthogonal frequency-division multiplexing (OFDM) is a widely used method of data transmission due to its various inherent advantages. In recent years, the possibility of using the OFDM waveform for radar purposes has gained an increasing amount of attention, and has become an active area of research. The method of Discrete Fourier Transform Spread (DFT-S) can be used to reduce the undesirable high peak-to-average power ratio (PAPR) inherent in the OFDM scheme, which is one of its main drawbacks. In this paper, the effect of the DFT-S technique on a radar system using the OFDM waveform is investigated. It is shown, through simulations performed in MATLAB, that the radar's performance is improved by the use of DFT-S in the transmitter. This suggests the compatibility of the OFDM waveform for both communications and radar applications.**

***Index Terms*—OFDM, radar, reciprocal filtering, peak-to-average power ratio (PAPR)**

I. Introduction

The prospect of combining radar and communication functionality into a single system is attractive for a few reasons. Firstly, the combined system would likely require less hardware, since both functions - radar and communications - could share certain hardware components, such as transmit and receive antennas, modulators, radio-frequency (RF) oscillators etc. The reduced amount of hardware would also help to reduce production cost, something which is especially important when it comes to mass production. Secondly, by combining the two systems into one, there is the opportunity to more efficiently use the frequency spectrum. This potential benefit is promising given the increasing investment in the Internet-of-Things (IoT) sector, where more and more devices are wireless-based, and integrated into single systems. And this question about the feasibility of combining the two functions into a single system is a somewhat natural one; many of the systems that use radar technology also require communications capabilities, like with the automobile industry or industrial automation sector. Moreover, both radar and wireless communication systems are based on the principle of transmitting and receiving electromagnetic (EM) waves. For wireless communications, orthogonal frequency-division multiplexing (OFDM) is a method of data transmission that is very often employed. This is because OFDM has many advantages, such as an efficient implementation using the Fast Fourier Transform (FFT) algorithm, a high spectral efficiency, and its robustness to interference and frequency-selective channels. Due to the widespread use of the OFDM waveform in 4G and 5G communication systems, its potential use in radar applications has received a lot of attention and been an active area of research for many years.

The layout of the rest of the paper is as follows: In section II, some background information about the method of DFT spreading and reciprocal filtering is given. In section III, a comparison and discussion of the simulation results is presented. Lastly, section IV discusses the conclusions, and offers some areas to possibly explore in future work.

II. Background

A. DFT-spread Technique

One of the main drawbacks of the OFDM waveform is its high peak-to-average power ratio (PAPR), which is caused by the Inverse Fast Fourier Transform (IFFT) block used in the transmitter (Tx). This high PAPR requires the high-power amplifier (HPA) used by the transmitter to have a highly linear characteristic, so as to avoid distortions of the waveform during transmission. Distortion of the waveform during transmission is very undesirable as it can lead to an increase in the communication system's bit error rate. As well as distortions, the high PAPR of the waveform can lead to a high power consumption in the user equipment (UE) used during uplink transmissions. A high power consumption can pose a challenge to the battery life of small and mobile devices. Various methods to combat the high PAPR of the OFDM waveform have been analysed in the literature. Some examples of the more common methods are selective mapping (SLM) [1], [2], tone reservation (TR) [3], tone injection (TI), and the Discrete Fourier Transform Spread (DFT-S) technique [4], [5]. The last method mentioned, DFT-Spread (DFT-S), is a point of focus in this paper.

The DFT-S technique involves first passing the set of transmit symbols - got from a Q-ary alphabet like QAM or QPSK - through a Discrete Fourier Transform (DFT) block, *before* they are mapped to the inputs of an Inverse Discrete Fourier Transform (IDFT) block. The DFT and IDFT operations are computed very efficiently using FFT and IFFT algorithms. Fig. 1 shows a basic block diagram for a DFT-S OFDM system.

The DFT-S technique works on the basis that the size of the DFT and IDFT blocks are different - if they were the same then the IDFT operation would cancel or negate the DFT's effect. The DFT block helps to mitigate the effect of the IDFT block (OFDM modulator) which is responsible for the high PAPR. The size of the IDFT block (L) is chosen to be an integer (K) multiple of the size of the DFT block - i.e., $L = KN$. This means one has some choice when mapping the N

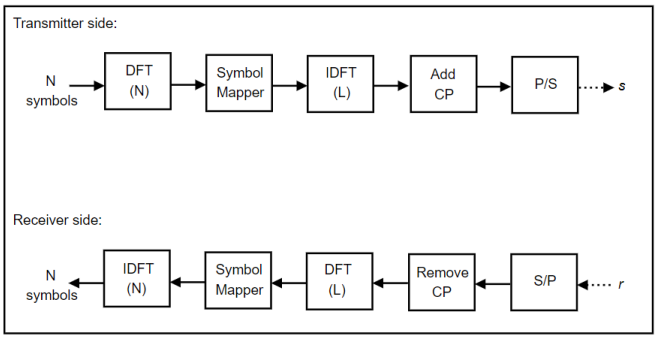

Fig. 1. Basic block diagram of a DFT-S OFDM System.

DFT outputs to the L IDFT inputs. Two mapping rules often used are interleaving and localised [6], [7]. Fig. 2 and 3 show the basic characteristics of the methods of interleaving and localised mapping.

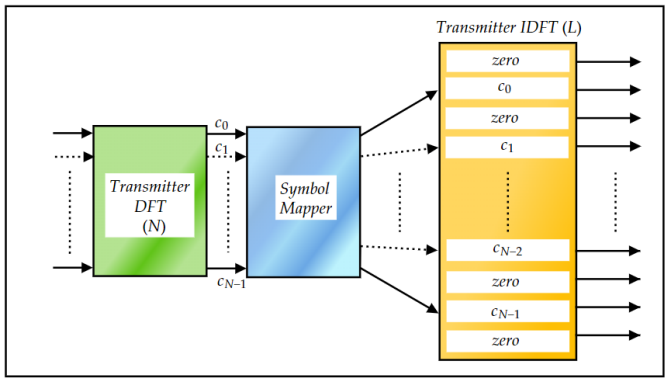

Fig. 2. Illustration of the idea of Interleaving Mapping.

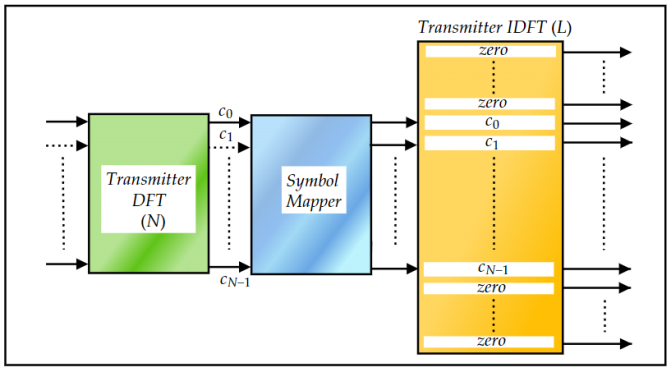

Fig. 3. Illustration of the idea of Localised Mapping.

When interleaving mapping is used, the N output symbols from the DFT block are mapped over the whole set of L IDFT inputs, and the data symbols [c_0, c_1, c_2,..., c_{N-1}] are equally spaced out, with an appropriate number of zeros in between - for example, a single zero is inserted between each of the symbols in Fig. 2 above.

B. OFDM transmit and receive sequences

1) The transmit sequence: An OFDM signal is a burst of OFDM symbols, where each OFDM symbol is itself composed of a number of mutually orthogonal subcarrier signals. Some subcarrier channels are often left idle, such as the DC subcarrier, while most are loaded with complex symbols. These symbols are either carrying information, or are acting as pilot symbols to be used for purposes such as channel estimation. Mathematically, an OFDM signal with M symbols, each using N subcarriers, may be represented in discrete time by (1)

$$s[l] = \sum_{m=0}^{M-1} \left(\frac{1}{\sqrt{N}} \sum_{n=0}^{N-1} c_{n,m} e^{-j2\pi \frac{n}{N}(l-mP)} \right) \quad (1)$$

In (1), $c_{n,m}$ represents the complex symbol that is loaded onto subcarrier channel n of OFDM symbol m. And l is the discrete-time index variable, while P is the extended OFDM symbol length after the cyclic prefix (CP) has been added on - i.e., $P = N + GN$, with G representing the fraction of the OFDM symbol length (N) used as a cyclic prefix or guard interval; typically values for G are $1/4$, $1/8$, and $1/16$.

2) The reflected signal: The reflected signal off a moving target is a delayed-in-time and shifted-in-frequency version of s, and can be expressed by (2)

$$r[l] = \alpha s[l - d_0] e^{j2\pi f_D \frac{l}{P}} + z[l] \quad (2)$$

Where α represents the signal attenuation caused by the target, f_D represents the *Doppler shift* caused to s by the moving target, and d_0 is the propagation delay associated with r, in units of samples. As is also shown in (2), the reflected signal is corrupted by additive White Gaussian noise, which is represented by z.

C. Reciprocal Filter

Correlation-based OFDM radar receivers have been analysed and discussed before, such as in [8], [9], and [10]. In most cases, the propagation delay, d_0, and Doppler shift, f_D, of the received signal, r, is obtained by computing a two-dimensional cross correlation between the received sequence and shifted replicas of the transmitted sequence

$$\chi_{r,s}(d, f) = \sum_{l=0}^{NM-1} r[l] s^*[l - d] e^{-j2\pi f \frac{l}{P}} \quad (3)$$

The expression in (3) is also known as the *ambiguity function*, and is used for analysing radar signals. By computing the correlation value, $\chi_{r,s}$, at various values of (d, f) a heat map or surface plot can be generated. Peaks in the heat map or surface plot correspond to signals which correlate highly with the received signal. From these peaks, estimates of the delay and Doppler shift in r can be made. The two-dimensional cross correlation in (3) can also be computed in a block-by-block manner by first converting the received sequence, r, into a matrix of M columns and N rows. This is another way of viewing the transmitted and received sequences that is discussed in detail in [11], and [12].

$$\mathbf{F_{Rx}} = \begin{pmatrix} b_{0,0} & b_{0,1} & \cdots & b_{0,M-1} \\ b_{1,0} & b_{1,1} & \cdots & b_{1,M-1} \\ \vdots & \vdots & \ddots & \vdots \\ b_{N,0} & b_{N,1} & \cdots & b_{N,M-1} \end{pmatrix} \quad (4)$$

With regards to (4), $b_{1,1}$ represents the received complex symbol on the second subcarrier channel of the second received OFDM symbol in the sequence r. Similarly, the transmitted sequence s can be re-expressed in this matrix format as shown in (5)

$$\mathbf{F_{Tx}} = \begin{pmatrix} c_{0,0} & c_{0,1} & \cdots & c_{0,M-1} \\ c_{1,0} & c_{1,1} & \cdots & c_{1,M-1} \\ \vdots & \vdots & \ddots & \vdots \\ c_{N,0} & c_{N,1} & \cdots & c_{N,M-1} \end{pmatrix} \quad (5)$$

Now the two-dimensional correlation can be computed on the corresponding columns in $\mathbf{F_{Tx}}$, and $\mathbf{F_{Rx}}$. Let s_m be the m-th transmitted OFDM symbol, and r_m be the m-th received OFDM symbol - i.e.,

$$s_m = [c_{0,m}, c_{1,m}, c_{2,m}, ..., c_{N-1,m}] \quad (6)$$

$$r_m = [b_{0,m}, b_{1,m}, b_{2,m}, ..., b_{N-1,m}] \quad (7)$$

The two-dimensional correlation between the two sequences shown in (6) and (7) can be expressed as in (8)

$$\chi_m(d, f) = \sum_{l=0}^{N-1} r_m[l] s_m^*[l-d] e^{-j2\pi f \frac{l}{P}} \quad (8)$$

Fig. 4 tries to illustrate the segmentation of the transmit and receive sequences into M symbols or "blocks". When (8) is

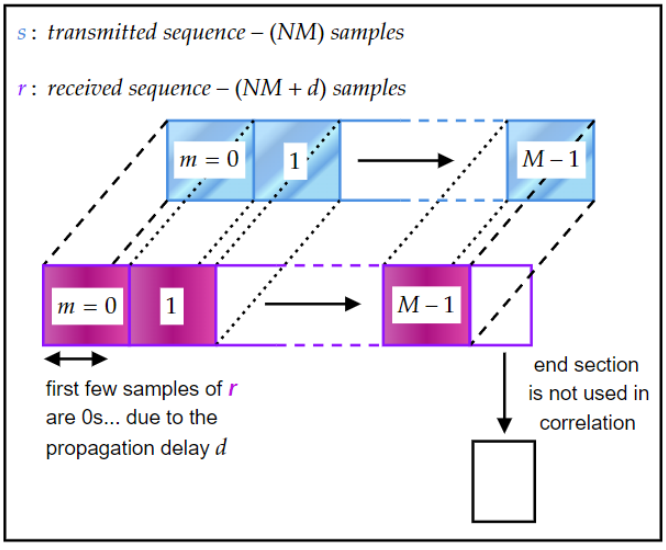

Fig. 4. Segmentation of the transmit and receive sequences to more easily allow for block-by-block processing.

computed for each of the M symbols, a new intermediate matrix is obtained with (M) rows, and $(2N-1)$ columns - where $(2N-1)$ is the length of the correlation sum between any s_m and r_m sequences.

$$\chi^{'}(d, f) = \begin{pmatrix} e_{0,0} & e_{0,1} & \cdots & e_{0,2N-1} \\ e_{1,0} & e_{1,1} & \cdots & e_{1,2N-1} \\ \vdots & \vdots & \ddots & \vdots \\ e_{M-1,0} & e_{M-1,1} & \cdots & e_{M-1,2N-1} \end{pmatrix} \quad (9)$$

The rows of this matrix can then be used to obtain the overall two-dimensional correlation of the sequences s and r, as indicated in (10).

$$\chi_{r,s}(d, f) = \sum_{m=0}^{M-1} \chi_m^{'}(d, f) e^{-j2\pi f m} \quad (10)$$

Fig. 5 shows an example of a heat map generated by computing (10). The simulation was done in MATLAB, and the simulation parameters are contained in Table I. So far, the

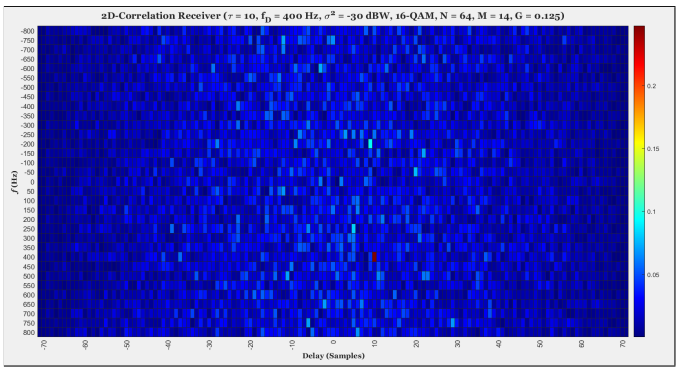

Fig. 5. Heat map generated from the correlation-based receiver defined by (8) and (10).

Number of subcarriers (N)	64
Number of OFDM symbols (M)	14
Modulation alphabet	16-QAM
Fraction of symbol used as CP (G)	1/8
Noise power (dBW)	-30
Signal attenuation (α)	2e-3

TABLE I. Simulation Parameters for Fig. 5.

correlation-based radar receiver discussed in this paper has been based on the (cross) ambiguity function. The reciprocal filter receiver is discussed and analysed in [8]. It is also analysed in [9], and [10] under the acronyms *MCC* and *CHAD*. To obtain the expression for the reciprocal filter only a small change in (8) is needed: instead of directly using the symbols of the transmit sequence (s), the reciprocal of each symbol or block (s_m) is first taken. Let the new sequence be denoted by $s_m^{'}$, where

$$s_m^{'} = 1/s_m^* \quad (11)$$

This new sequence, $s_m^{'}$, then replaces s_m in (8).

III. Comparison of Results

In this section, the effect of using DFT-S with the reciprocal filter receiver is analysed. The number of subcarriers (N) and the number of OFDM symbols (M) in the transmit sequence are varied, as well as the noise power. It is seen that the use of DFT-S leads to an improved performance in each of the simulated scenarios. The effect of using interleaving and localised mapping schemes is also investigated.

A. Interleaving Mapping

First, the interleaving method of mapping will be considered. The simulation parameters that were used are shown in Table II. Fig. 6 shows the heat map generated by a reciprocal

Number of subcarriers (N)	16, 32, 54, 64
Number of OFDM symbols (M)	7, 10, 14
Modulation alphabet	16-QAM
Fraction of symbol used as CP (G)	0, 1/8
Noise power (dBW)	-25, -30, -40
IDFT size (L)	$2N$, $4N$
Signal attenuation (α)	2e-3

TABLE II. Simulation Parameters used in MATLAB Simulations.

filter receiver. The number of subcarriers (N) used was 64, and a total of 7 OFDM symbols were in the transmit sequence. The modulation scheme used was 16-QAM, and G was chosen to be 1/8. As can be seen in Fig. 6, it is not easy to discern the

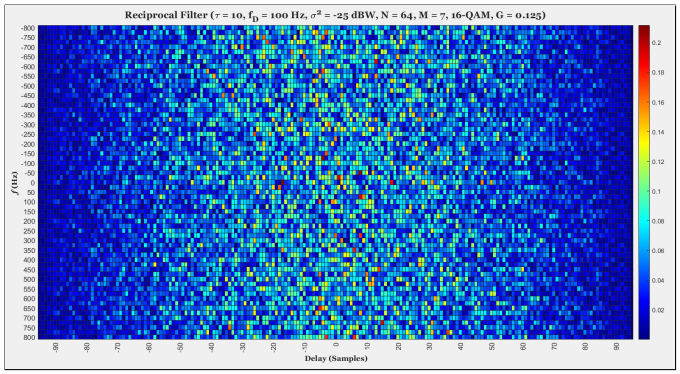

Fig. 6. Reciprocal filter radar receiver, with no DFT-S on the transmit side.

peak in the heat map located at the simulated delay (d_0) of 10 samples and Doppler shift (f_D) of 100 Hz. Considering Fig. 7, the red-coloured peak in the heat map is more easily picked out when the DFT-S technique is used. One promising advantage of the DFT-S technique on the transmitter side is the possibility of achieving an improved performance with a small number of data subcarrier channels (N) in use. Fig. 8 shows the heat map obtained when only 32 subcarriers are used ($N = 32$). It is seen that there is a strong correlation at a delay (d_0) of 10 samples, and a Doppler shift (f_D) of 100 Hz. However, there are some ambiguous peaks in the heat map, like in the previous case. This makes the decision-making process at the

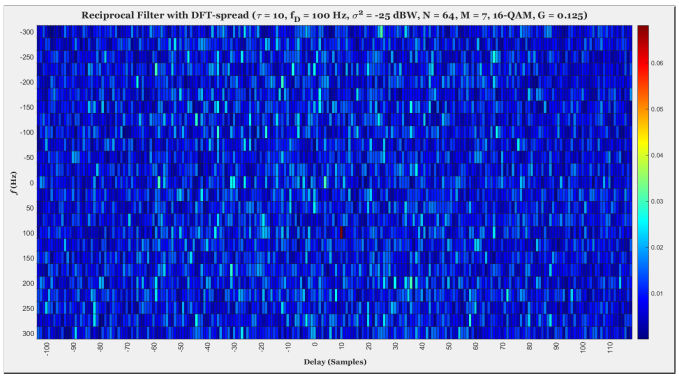

Fig. 7. Reciprocal filter radar receiver **with** DFT-S on the transmit side. Zoomed in to improve visibility.

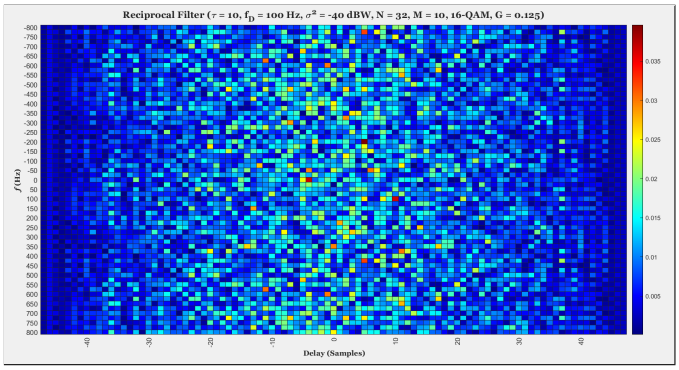

Fig. 8. Reciprocal filter radar receiver with no DFT-S on the transmit side.

receiver difficult. Comparing this with Fig. 9, it is seen that when DFT-S is implemented the red-coloured peak is much easier to spot in the resulting heat map. The size of the IDFT block (L) was set to be four times that of the DFT block - i.e., $L = 4N$. The DFT-S technique appears to have helped

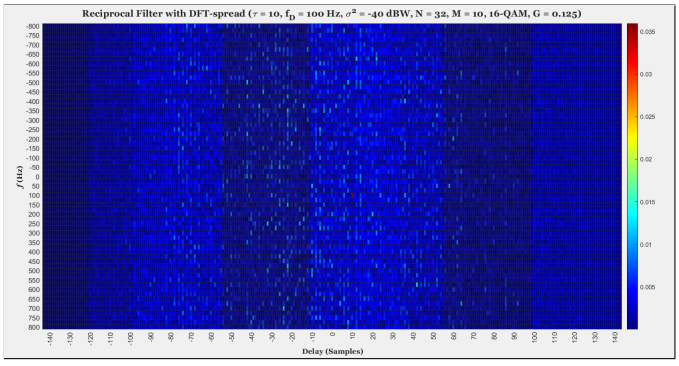

Fig. 9. Reciprocal filter radar receiver **with** DFT-S on the transmit side.

mitigate the effect of the additive White Gaussian noise. This would likely make the decision process for the radar receiver easier, and reduce the amount of post processing needed in

order to identify the correct delay (d_0) and Doppler shift (f_D) values.

B. Localised Mapping

Next, the effectiveness of localised mapping with the DFT-S technique will be investigated. In Fig. 10, the heat map obtained corresponds to when no DFT-S was employed at the transmitter. The number of subcarriers was set to 64 ($N = 64$), and 14 OFDM symbols were generated ($M = 14$). Like in the previous scenarios, 16-QAM was the modulation scheme used. The value of G was 1/8. In Fig. 10, it is seen that there

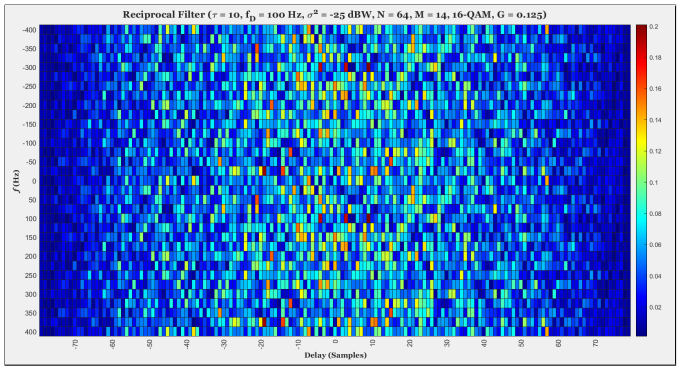

Fig. 10. Reciprocal filter with no DFT-S technique implemented on the transmitter side.

is a high correlation near the correct point ($d_0 = 10, f_D = 100$) in the heat map. However, there are other points of high correlation, which makes the decision-making process for the radar receiver harder in this instance. This is in contrast to Fig. 11, where the heat map generated after employing DFT-S has a much more discernible red peak at the point ($d_0 = 10, f_D = 100$). The IDFT size (L) was twice that of the DFT block (N).

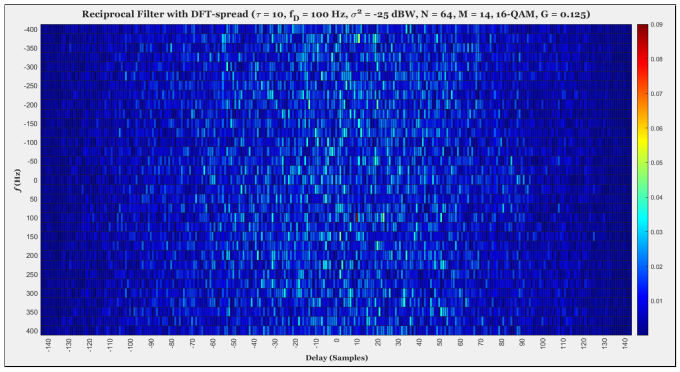

Fig. 11. Reciprocal filter **with** the DFT-S technique implemented on the transmitter side. $L = 2N = 128$.

It is worth illustrating that even with as few as 16 subcarriers in use, the DFT-S technique helps yield respectable results, while the standard reciprocal filter implementation without the transmit-side DFT-S produces a heat map with many ambiguities. Reducing the number of subcarriers would help reduce the transmit power required, and it would also reduce the bandwidth (B) of the OFDM radar system - these are often desirable attributes. Fig. 12 shows the results obtained when only 16 subcarriers are used ($N = 16$), and when the DFT-S technique is not implemented by the transmitter. As is seen

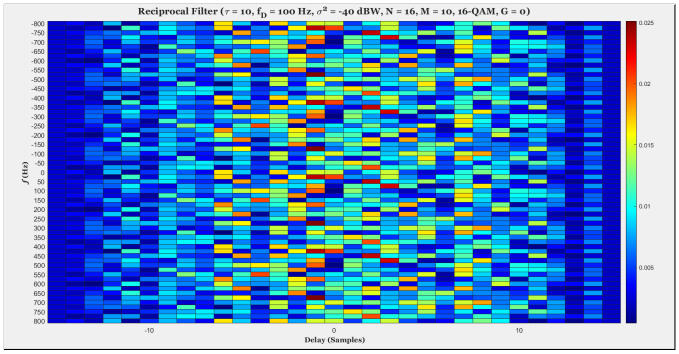

Fig. 12. Reciprocal filter with no DFT-S implemented, and only 16 subcarriers in use.

in Fig. 12, the performance of the reciprocal filter is degraded when the number of subcarriers in use is too low. The heat map obtained is insufficient for the receiver to establish the correct delay (d_0) and Doppler shift (f_D) associated with the received signal (r). Fig. 13 shows an improved result after DFT-S is

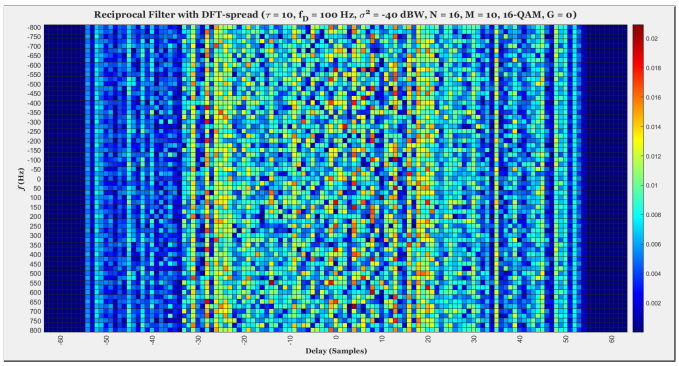

Fig. 13. Reciprocal filter with DFT-S implemented. Only 16 subcarriers in use.

employed by the transmitter, although it is still clear that the reduction in the number of subcarriers used has had a negative effect on the heat map generated. Lastly, it is worth illustrating that in some scenarios one can use less active subcarriers (N) with the DFT-S technique *and* achieve an equal or improved performance. Fig. 14 shows the heat map for a reciprocal filter, without DFT-S used at the transmitter. The number of subcarriers (N) in use was 64. Comparing this with Fig. 15, which shows the heat map obtained when $N = 16$ and DFT-S is used, it is seen that the performance is no better in the first instance, when the number of subcarriers was 64 ($N = 64$).

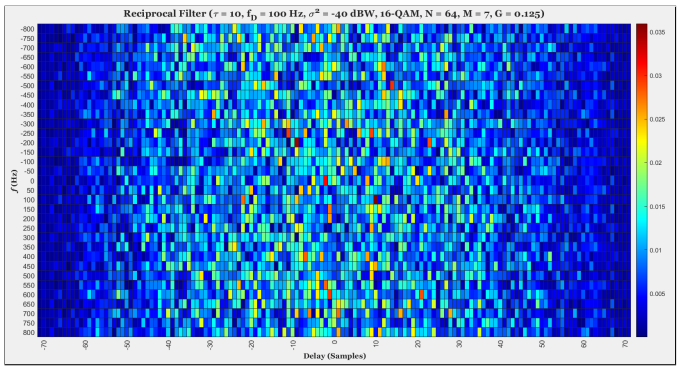

Fig. 14. Reciprocal filter with **no** DFT-S implemented, and **64** subcarriers in use.

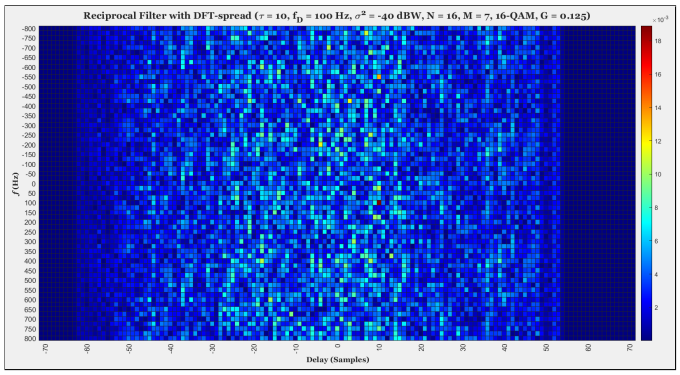

Fig. 15. Reciprocal filter **with** DFT-S implemented, and **16** active subcarriers in use.

IV. Conclusions and Future Work

In this paper it was shown that the performance of an OFDM radar system - based on the reciprocal filter receiver - can be improved by use of a DFT-spread stage in the transmitter chain. This is promising for various reasons:

- The peak-to-average power ratio (PAPR) of the radar signal can be reduced without compromising the radar's performance, owing to the implementation of the DFT-Spread stage in the transmitter chain.
- The DFT-Spread stage puts less demand on the transmitter's high-power amplifier. This reduces the hardware cost, as the resulting amplifiers are easier and less expensive to build.
- The DFT-Spread technique is already in use in wireless communications, and so it is promising to see that the radar's performance is not hindered by its inclusion in the transmitter chain. It also gives promise to the idea of combining both communications and radar functionality into a single system, which would bring many advantages, as discussed in the introduction.
- The scenarios simulated in this paper suggest that one can use a lower number of active subcarriers (N) and achieve a better performance when the DFT-Spread technique is used (cf. Fig. 14 and 15).
- With localised mapping, the edge subcarriers are left idle. This can help protect against interference from other systems that use a similar section of the frequency spectrum.

Some areas to explore in future work might be:

- Investigate the effectiveness of the DFT-S technique with other OFDM radar receivers, such as ones that are based on the periodogram.
- Investigate other mapping techniques. For example, the distributed method of mapping the outputs from the DFT block to the inputs of the IDFT block.
- Analyse the results when different modulation alphabets are used, such as 64-QAM, 16-QPSK, or BPSK.

References

[1] Khaled Tani, Yahia Medjahdi, Hmaied Shaiek, Rafik Zayani, and Daniel Roviras. Papr reduction of post-ofdm waveforms contenders for 5g amp; beyond using slm and tr algorithms. In *2018 25th International Conference on Telecommunications (ICT)*, pages 104–109, 2018.

[2] N. Ohkubo and T. Ohtsuki. Design criteria for phase sequences in selected mapping. In *The 57th IEEE Semiannual Vehicular Technology Conference, 2003. VTC 2003-Spring.*, volume 1, pages 373–377 vol.1, 2003.

[3] Filippo Tosato, Magnus Sandell, and Makoto Tanahashi. Tone reservation for papr reduction: An optimal approach through sphere encoding. In *2016 IEEE International Conference on Communications (ICC)*, pages 1–6, 2016.

[4] M. F. Pervej, M. Z. I. Sarkar, T. K. Roy, M. M. Hasan, M. M. Rahman, and S. K. Bain. Analysis of papr reduction of dft-scfdma system using different sub-carrier mapping schemes. In *2014 17th International Conference on Computer and Information Technology (ICCIT)*, pages 435–439, 2014.

[5] Rizwana Ahmad and Anand Srivastava. Papr reduction of ofdm signal through dft precoding and gmsk pulse shaping in indoor vlc. *IEEE Access*, 8:122092–122103, 2020.

[6] Zi-Yang Wu, Gao Yu-Liang, Ze-Kun Wang, Chuan You, Chuang Yang, Chong Luo, and Jiao Wang. Optimized dft-spread ofdm based visible light communications with multiple lighting sources. *Optics Express*, 25:26468, 10 2017.

[7] Khaled Tahkoubit, Adda Ali-Pacha, Hmaied Shaiek, and Daniel Roviras. Papr reduction of bf-ofdm waveform using dft-spread technique. In *2019 16th International Symposium on Wireless Communication Systems (ISWCS)*, pages 406–410, 2019.

[8] Steven Mercier, Stéphanie Bidon, Damien Roque, and Cyrille Enderli. Comparison of correlation-based ofdm radar receivers. *IEEE Transactions on Aerospace and Electronic Systems*, 56(6):4796–4813, 2020.

[9] Stephen Searle, James Palmer, Linda Davis, Daniel W. O'Hagan, and Martin Ummenhofer. Evaluation of the ambiguity function for passive radar with ofdm transmissions. In *2014 IEEE Radar Conference*, pages 1040–1045, 2014.

[10] Ghislain Gassier, Gilles Chabriel, Jean Barrère, Françoise Briolle, and Claude Jauffret. A unifying approach for disturbance cancellation and target detection in passive radar using ofdm. *IEEE Transactions on Signal Processing*, 64(22):5959–5971, 2016.

[11] Klaus Martin Braun. *OFDM radar algorithms in mobile communication networks*. PhD thesis, Karlsruhe, Karlsruher Institut für Technologie (KIT), Diss., 2014, 2014.

[12] Martin Braun, Christian Sturm, and Friedrich K. Jondral. Maximum likelihood speed and distance estimation for ofdm radar. In *2010 IEEE Radar Conference*, pages 256–261, 2010.